Control Engineering Practice 38 (2015) 11–25

Contents lists available at ScienceDirect

Control Engineering Practice

journal homepage: www.elsevier.com/locate/conengprac

Experimental evaluation of decentralized cooperative cruise control for heavy-duty vehicle platooning

Assad Alam [a,b,*], Jonas Mårtensson [b], Karl H. Johansson [b]

[a] Scania CV AB,SE-15187 Södertälje, Sweden
[b] ACCESS Linnaeus Centre, Royal Institute of Technology, 100 44 Stockholm, Sweden

ARTICLE INFO

Article history:
Received 9 April 2014
Accepted 11 December 2014

Keywords:
Heavy-duty vehicle
Platooning
Linear quadratic control
Vehicle-to-vehicle communication
Adaptive intelligent cruise control

ABSTRACT

In this paper, we consider the problem of finding decentralized controllers for heavy-duty vehicle (HDV) platooning by establishing empiric results for a qualitative verification of a control design methodology. We present a linear quadratic control framework for the design of a high-level cooperative platooning controller suitable for modern HDVs. A nonlinear low-level dynamical model is utilized, where realistic response delays in certain modes of operation are considered. The controller performance is evaluated through numerical and experimental studies. It is concluded that the proposed controller behaves well in the sense that experiments show that it allows for short time headways to achieve fuel efficiency, without compromising safety. Simulation results indicate that the model mimics real life behavior. Experiment results show that the dynamic behavior of the platooning vehicles depends strongly on the gear switching logic, which is confirmed by the simulation model. Both simulation and experiment results show that the third vehicle never displays a bigger undershoot than its preceding vehicle. The spacing errors stay bounded within 6.8 m in the simulation results and 7.2 m in the experiment results for varying transient responses. Furthermore, a minimum spacing of -0.6 m and -1.9 m during braking is observed in simulations and experiments, respectively. The results indicate that HDV platooning can be conducted at close spacings with standardized sensors and control units that are already present on commercial HDVs today.

1. Introduction

1.1. Motivation

The transport industry faces great challenges. Freight transport demand has escalated and will continue to do so as economies grow. At the same time legislation on engine emissions is becoming increasingly stringent. 2.3 billion tonne-kilometers of inland freight was transported in 2010, of which 76.4% was transported over roads. Overall green house gas emissions was recorded to be reduced by 17% between 1990 and 2009 (Eurostat, 2011). While emissions from other sectors are falling, those from the transport sector have increased by 21%. Road transport alone contributes about 20% of the EU's total emissions of CO_2, the main greenhouse gas. Congestion is a growing problem, being a natural consequence of the increasing need for transport services. Along with challenges regarding congestion and emission policies, the vehicle manufacturers also experience an increase in fuel prices. Transportation is responsible for the main part of the increase in oil consumption during the last three decades, and the growth is expected to continue. As the fuel price increases, the strain on operating costs grows for a heavy-duty vehicle (HDV) fleet provider. This issue has a major impact within the transport industry, since road transport serves as the backbone of the economy in many countries. With the rise in fuel prices, road transportation becomes less economically viable. Hence, the road transport sector has been targeted as a main policy area where further environmental and overall efficiency improvements are critical for a sustainable future of European transport (European Commission, 2014).

The advancements in information and communication technology (ICT) present an opportunity to tackle these problems through novel integrated intelligent transportation system (ITS) solutions. Through improved sensor technology, wireless communication, GPS devices, and digital maps, advanced driver assistance systems are being developed. Key enabling technologies, such as vehicle-to-vehicle (V2V) and vehicle-to-infrastructure (V2I) communication, have matured. Furthermore, the number of on-board electronic control units (ECUs) and sensors have increased rapidly over the last decades. They enable additional functionality in terms of smart control logics.

HDV platooning for emission reduction and energy efficiency is intensively studied. It is known that driving at a short inter-vehicle

* Corresponding author at: ACCESS Linnaeus Centre, Royal Institute of Technology, 100 44 Stockholm, Sweden.
E-mail addresses: assad.alam@scania.com, assada@kth.se (A. Alam), jonas1@kth.se (J. Mårtensson), kallej@kth.se (K.H. Johansson).

http://dx.doi.org/10.1016/j.conengprac.2014.12.009
0967-0661/

spacing to a vehicle ahead results in a reduced fuel consumption and drivers are doing so today with increased stress levels. The reduced fuel consumption occurs due to a lowered air drag when operating in a formation, which in turn creates a coupling of the dynamics between vehicles throughout the platoon. By packing HDVs close to each other, the total road capacity can be increased and emissions can be reduced (De Schutter et al., 1999). Additionally, when governing vehicle platoons by an automated control strategy, accidents can be reduced and the overall traffic flow is expected to improve (Ioannou & Chien, 1993). It is fuel efficient to minimize the relative distance between the vehicles to achieve maximum reduction in air drag (Alam, Gattami, & Johansson, 2010), but, as traffic intensity grows, the complexity of the coupled traffic dynamics increases. The actions of one vehicle may in turn affect all vehicles in a linked chain.

Research projects throughout the world have been conducted to study the challenges and benefits of HDV platooning in practice. In the projects PROMOTE-CHAUFFEUR I & II, needs of intermediate and end users, along with safety and operational requirements, were investigated (Harker, 2001). In KONVOI, experimentally analyzing the use of electronically regulated truck convoys on the road with five vehicles was one of the main focuses (Deutschle et al., 2010). PATH is a vast project that addresses many traffic related research aspects (Bu, Tan, & Huang, 2010). Recently, the focus has been directed towards studying HDV platooning, mainly due to the fuel and congestion reduction potential. The recently concluded ENERGY ITS project evaluated energy efficiency for automated HDV platooning and methods for effectiveness of ITS on energy saving (Tsugawa, 2013). In the SARTRE project, the focuse lied on mixed traffic in highway situations, where fuel efficiency, safety, and comfort were evaluated (Robinson, Chan, & Coelingh, 2010). The aim of the GCDC project was to accelerate the deployment of cooperative driving systems (van Nunen, Kwakkernaat, Ploeg, & Netten, 2012). Several issues, such as communication constraints and erroneous information, were revealed in this project that needs to be solved before platooning can be presented commercially. Finally, in the recent project COMPANION (Adolfson, 2014) a wider perspective is undertaken, where the actual creation, coordination, and operation of platoons are studied. The goal is to identify means of applying the platooning concept in practice for daily transport operations.

There are already commercially available systems that might facilitate platooning, such as the adaptive cruise control (ACC) that uses radar measurements consisting of the relative distance and velocity to a preceding vehicle and adjusts the velocity automatically. The ACC works reasonably well in a two-vehicle platoon. However, a delay arises from measuring the behavior of the preceding vehicle with the radar to producing the actual brake torque at the wheels. Thus, overshoots commonly occur when facing a velocity disturbance. In addition, the follower vehicle might not be able to reduce its speed in time if the preceding vehicle performs an emergency brake. Therefore, it is not suitable for longer vehicle platoons to operate at a short spacing due to safety issues. As an alternative to radar measurements, wireless communication may be utilized to provide information from several preceding vehicles. Even though small delays are still imposed due to data processing, retransmissions, etc., the vehicles should be able to operate at much closer spacing and better performance with a suitable controller, since a wider range of information, e.g., braking events or other actions performed by several vehicles ahead, can be transmitted almost instantaneously.

1.2. Contribution

The main contribution of this paper is to derive a decentralized controller for HDV platooning and establish empiric performance results for the presented control design. Several studies on vehicle platooning have been based on simplified theoretical models. However, as shown in this paper, delays and nonlinear dynamics can significantly influence the closed-loop system. In Alam, Gattami, and Johansson (2011), an early version of the proposed controller design was given, where only one preceding vehicle in the platoon was considered. In this work, we present a method for designing suboptimal decentralized feedback controllers for an arbitrary number of preceding vehicles, with low computational complexity, that also takes dynamic coupling and engine response delays into consideration. The controller performance is evaluated through implementation on commercial HDVs. The design method is scalable in the sense that an additional vehicle can be added at the tail of the platoon without mandating a change in the controllers of the already platooning vehicles. Our proposed vehicle system architecture is shown to be robust to packet losses or short outages in V2V communication. As modern HDVs in general have two separate low-level control systems for governing the longitudinal propulsion and deceleration of the vehicle, the engine management system (EMS) and the brake management system (BMS), we present a simple bumpless transfer scheme to switch between these systems. The proposed platooning controller can be easily implemented on modern HDVs without requiring any changes in the already existing vehicle architecture. It includes three modes, where two modes involve maintaining a suitable distance when facing disturbances during normal operation mode. The third mode incorporates the control strategy derived in Alam, Gattami, Johansson, and Tomlin (2014), which was solely derived for collision avoidance during emergency braking scenarios. We present a suitable vehicle control architecture that also takes existing commercially available speed control strategies into account and we give test procedures for performance evaluation. We show that the controller behaves well even when performing outside the linear region of operation. We also show that the proposed controller attenuates the effect of disturbances downstream in the platoon, when studying scenarios that commonly occur on highways with dynamic operating conditions and physical constraints. Experimental results are given to qualitatively validate the proposed control system behavior. The results show that the controller performance is improved with increasing position index in the platoon, by utilizing additional information from preceding vehicles. However, the effects of unmodeled nonlinearities, such as gear changes, brake blending, and engine dynamics, can cause undesirable behavior in some cases. The experiments have been conducted on a test site south of Stockholm, using HDVs provided by Scania CV AB.

1.3. Related work

A multitude of control strategies for vehicle platooning can be found in the literature since the 1950s. For brevity, we only outline some of the theoretical work on vehicle platooning and more recent literature on implementation and experiments.

1.3.1. Fundamentals of vehicle platooning

Fundamentals of vehicle platooning are well researched and involve stabilizing control based on simple point mass models, string stability, safety, and traffic flow. Early theoretical work on control of vehicular platoons was done by Levine and Athans (1966). Centralized linear quadratic regulator (LQR) design for vehicle platoons was considered in this work, indirectly assuming that computational complexity and V2V communication constraints would not be an issue. In Jovanović and Bamieh (2004), it was shown that even though infinite platoons capture the essence of large platoons, the LQR problem formulation lacks observability and stabilizability in the infinite case. Hence, a well-posed alternative formulation for large vehicle platoons is proposed. Control for chain structures in the context of platoons

has been studied through various perspectives, e.g., in Dunbar and Murray (2006) based on following a predecessor and in Barooah, Mehta, and Hespanha (2009) based on bidirectional schemes. It has been shown that control performance may vary depending on the available information within the platoon. A survey on platooning and inter-vehicle control is given in Kavathekar and Chen (2011).

Platooning controllers can be viewed as an extension to the ACC concept and thereby be categorized based upon their intra-platoon spacing policies. Either a constant spacing is used (Swaroop, Hedrick, Chien, & Ioannou, 1994), a time headway (Chien & Ioannou, 1992), or a nonlinear spacing policy (Yanakiev & Kanellakopoulos, 2008). In Omae, Fukuda, Ogitsu, and Chiang (2013), it is shown that a time headway policy results in a more energy efficient control, since constant spacing policy requires a higher acceleration variability for handling disturbances. The disadvantage with having a constant time headway is that it results in larger steady-state spacing, which increases the platoon length and thereby decreases the benefits from the air drag reduction along with the traffic throughput. Thus, two nonlinear policies were introduced in Yanakiev and Kanellakopoulos (2008), where the first policy is a variable time headway that varies linearly with the relative velocity error and the second policy is a nonlinear function of the separation error. It is concluded that the policies need to be evaluated in practice, since they add to the computational complexity and result in a trade-off between platoon performance, control smoothness, and robustness.

String stability for vehicle platoons is an important concept. It addresses the ability to suppress a disturbance in position, velocity, or acceleration, as it propagates along the platoon. Focusing on preventing collisions, the errors in spacing between the vehicles in the platoon are often considered. Early work on string stability can be found in Peppard (1974). In Swaroop and Hedrick (1996), a mathematical definition of string stability is introduced. It is not possible to achieve longitudinal string stability with a constant spacing policy for a homogeneous string of vehicles with feedback control based on nearest neighbor communications, see Sheikholeslam and Desoer (1993). In Seiler, Pant, and Hedrick (2004) it was shown that this limitation occurs due to a complementary sensitivity integral constraint. Hence, it is preferable to use a time headway spacing both with respect to string stability and energy efficiency. In Middleton and Braslavsky (2010), communication constraints are considered in a chain of linear time-invariant autonomous vehicles with sufficient conditions for string stability being given. String stability can also be obtained in some cases through an ordering strategy with respect to vehicle mass (Liang, Alam, & Gattami, 2011). In Kianfar, Falcone, and Fredriksson (2013) string stability is studied in a lateral direction and in Knorn and Middleton (2013), it is studied in both continuous time and discrete position within the string. Ensuring string stability does not however always guarantee safety. If a collision occurs due to a harsh braking by any vehicle in the platoon, a collision can still occur downstream. Hence, in Alam et al. (2014), a possible framework is presented for analyzing collision avoidance in HDV platooning. Safety sets are given in the spacing and relative velocity, which are validated through empirical findings.

1.3.2. Implementation and evaluation of vehicle platooning

Vehicle platooning is in practice implemented through the EMS and BMS. Similarly, the conventional cruise control system (CC) in modern vehicles receives a set speed and utilizes the EMS to compute the required engine torque for maintaining the velocity (Shaout & Jarrah, 1997). However, an HDV commonly accelerates over steep downhill segments even though no engine torque is applied, due to its extensive mass. In addition, it is often not able to maintain the speed when traversing an uphill segment even though maximum engine torque is applied. The downhill speed control (DHSC) is a function specially developed for HDVs that prohibits the vehicle from exceeding a certain offset in speed when using the CC. With the aid of, for example, map data, the use of the DHSC can be minimized by adjusting the speed based on the vehicle characteristics. Thereby, the fuel consumption can be reduced (Hellström, 2010). The ACC has been considered as a means to enable vehicle platooning in Hedrick, McMahon, Narendran, and Swaroop (1991) and Rajamani and Zhu (1999). It generally acts as an extension to the CC, with the addition of actuating the vehicle with the brake system. Thus, the complexity of the control design increases, in particular for an HDV, since the EMS and BMS are typically very different nonlinear controllers with significantly different control input saturations. A maximum engine torque of 3000 N m can generally be produced by a strong HDV engine, whereas the maximum brake torque is typically 60 000 N m per axle.

In HDV platooning, mass and road slope has a significant effect on the system dynamics. Naus, Vugts, Ploeg, van de Molengraft, and Steinbuch (2009) presented a setup for cooperative ACC (CACC) for which feasibility of the actual implementation was one of the main objectives. Another design approach for a practical CACC was presented in Bu et al. (2010). In Milanes et al. (2014), a control system is designed, which is evaluated on four production passenger cars and the performance is evaluated in comparison with the ACC. Both longitudinal and lateral control are designed and evaluated on a platoon of eight passenger vehicles in Rajamani, Tan, Law, and Zhang (2000), where experimental results obtained from a 12.2 km long highway are presented. Considering nonlinearities and powertrain actuator uncertainties in HDVs, a method for calculating worst case spacing bounds is given in Rödönyi, Gáspár, and Bokor (2013). In Lidström et al. (2012) and Mårtensson et al. (2012), system architectures, wireless communication, and control for platooning applications were studied and evaluated through experiments in mixed traffic on a highway. Fuel reduction potentials of 5–20% were demonstrated in experiments by Alam et al. (2010), Robinson et al. (2010), and Tsugawa (2013). These results indicate that HDV platooning is an attractive concept.

1.4. Outline

The outline of the paper is as follows. In Section 2, we present the control system architecture. The system model is given in Section 3. In Section 4 we develop a method for deriving the proposed decentralized controllers and then give a simple bumpless transfer scheme, based on performance and driver acceptance, for switching between the low-level EMS and BMS controllers. Simulation results are given in Section 5 to determine and evaluate the chosen weight parameters for the controller. The experimental setup based on three HDVs is presented in Section 6 together with the experimental results. Conclusions are given in Section 7. A preliminary version of this paper was presented as Alam et al. (2011), in which an early version of the decentralized LQR for a simple platooning model was presented.

2. Vehicle platoon control architecture

The objective of the platoon controller is to maintain a small inter-vehicle spacing for fuel efficiency, without compromising safety. In this section we first describe the communication requirements for HDV platooning control. Then a platooning system architecture and a vehicle system architecture are proposed.

2.1. Platoon system communication constraints

The system that we consider in this paper is a platoon consisting of N HDVs, as illustrated in Fig. 1, traveling on a road with a

given initial set speed and relative distance. Each vehicle is equipped with a radar and a wireless transceiver. The radar provides information regarding the preceding vehicle's distance and velocity and the V2V communication provides system state information, events, and vehicle parameters.

We consider a decentralized controller, mainly due to the communication constraints that occur in practice. Using a centralized controller implies that the global states and system parameters are known to every vehicle in the platoon. Thereby, a central unit, for example a vehicle in the platoon or a road side unit, determines the control actions for all the vehicles in the platoon. A centralized control scheme requires an increase in communication with the number of vehicles in the platoon. Furthermore, package drops or outages can occur in wireless transmission. A centralized system is sensitive to communication delays and physical limitations on the radio range. It is often not realistic to assume that every vehicle in the platoon knows the state of every other vehicle instantaneously due to physical constraints in the information flow. It is, however, reasonable to assume that a vehicle is able to communicate with some vehicles within a given range. Hence, a decentralized strategy is suitable, where every vehicle determines its own control actions based on local information.

2.2. Platoon system architecture

The platoon system architecture that we consider is illustrated in Fig. 2. The arrows indicate the direction of information flow in the system. Vehicle information is obtained through on-board sensors, which is used in feedback controller, as illustrated by the arrow from a vehicle to its controllers. The arrow between a preceding vehicle and the ACC shows the information that is obtained through the radar. Here, state information is provided with respect to the preceding vehicle. The arrows between each CACC and the wireless communication network show the two-way communication between the platooning vehicles. It includes the system state information and the vehicle parameter information.

We propose a layered control system architecture, as illustrated in Fig. 2. Starting from the bottom, the conventional CC offers three services: maintained vehicle speed, improved fuel economy, and driver comfort over long distances. It typically uses velocity feedback information and acts as a PI- or a PID-controller to determine the required change in velocity, which is then sent as an input to the low-level controllers. In case of system failure, the driver is instructed to take full control of the vehicle.

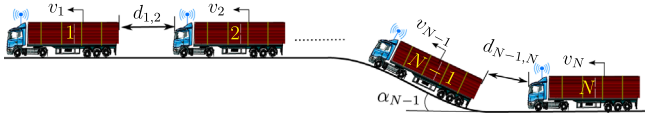

Fig. 1. A platoon of N HDVs traveling on a road with gradient α_i for vehicle i, inter-vehicle spacing $d_{i-1,i}$, and velocity v_i, where $i=1,\ldots,N$ is the vehicle position number in the platoon.

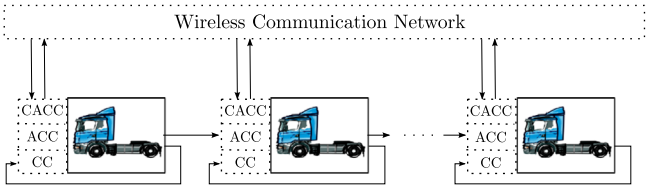

Fig. 2. Platoon system architecture for an N vehicle platoon. The lead vehicle, with index $i=1$, is to the left and the last vehicle is to the right. The control architecture for vehicle speed control is shown in front of each vehicle. The information flow in the system is given by the arrows.

The ACC, in the layer above, aims to maintain a desired spacing policy by utilizing relative distance and velocity information based on the preceding vehicle. It optimizes the control input with respect to fuel efficiency and driver comfort. Controllers typically allow for a reduced spacing during downhills such that unnecessary braking actions are avoided. Safety is improved since, as opposed to the CC, the ACC is allowed to actuate the brakes and can react faster than a driver. In case of system failure, the driver is warned and the control actions are degraded to the CC layer.

The CACC, in the top layer, is a cooperative adaptive cruise controller, which forms optimal decentralized decisions based on vehicles within spatial range of its wireless transceiver. The cost function includes the behavior of the surrounding vehicles, hence control actions are based on self-interest as well as the interests of all other vehicles in the platoon. Thus, the aim is to maintain a suitable inter-vehicle distance to several preceding vehicles with respect to fuel efficiency, robustness, and safety. By displaying a cooperative and synchronous behavior the inter-vehicle spacing can be reduced, thereby lowering the fuel consumption. Safety is improved by forming control actions based on preview information. If platooning constraints are imposed with respect to maximum acceleration and deceleration, controller actions might be implemented to further improve safety, comfort and fuel optimality. In the occurrence of a system failure in this layer, the control actions are degraded to the ACC layer.

There are several challenges in this architecture. The low-level controllers handle some of the nonlinearities in the vehicle and inherently linearize the vehicle behavior to some extent. However, a drawback is that the model uncertainty increases within the dynamic range of operation, since the behavior of the nonlinear low-level controllers might vary in behavior depending on its current state. For example, step responses of the same magnitude might vary depending on the current gear, if the engine was idling or active, or if the BMS was active just before the step is requested. Furthermore, radar information can be lost, for example in curves, when the preceding vehicle is not directly in front. Delays in wireless communication or in processing of radar information can occur, which must be handled by the active controller.

2.3. Vehicle system architecture

Each HDV has the system architecture shown in Fig. 3. Several control units are connected to the controller area network (CAN). The wireless sensor unit (WSU), GPS, and radar act as sensor units, providing information about the surrounding environment. Even though a wide range of information is available, from wireless communication, ECUs, and on-board sensors, it is often noisy and must be processed before it can be used as inputs to the controllers. In the data processing block, the noisy data from all the transmitting vehicles in the established platoon are processed

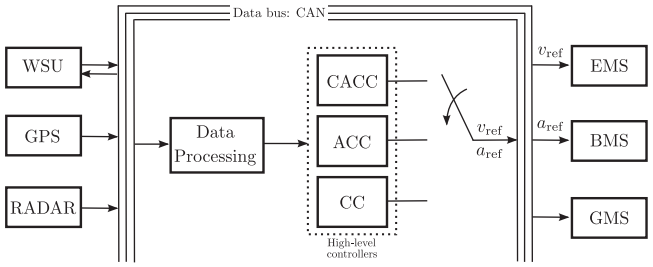

Fig. 3. Vehicle system architecture for the data processing and control. The arrows indicate the information flow that is shared through CAN. The driver chooses what controller to activate, which is indicated by the switch. If a failure occurs in the CACC when active, the system will automatically switch to the ACC and then to the CC if a failure in the ACC occurs.

through a Kalman filter and GPS information from the preceding vehicle is fused together with the state information from the radar. In the event of packet losses or short outages, the Kalman filter acts as a state predictor. Each received message from other platooning vehicles contains GPS information. Based on the position and heading of each surrounding vehicles, the platooning vehicles are mapped to a local coordinate system. Filtered information, along with vehicle specific parameters, controller gains, and the current mode of operation for the platooning vehicles, is forwarded to the high-level controllers block. The active controller sends out the reference signal on CAN, which is then carried out by the low-level controllers shown to the right in Fig. 3.

The low-level control systems consist of the EMS, BMS, and gear management system (GMS). The EMS controller receives a velocity request as an input. It then calculates the required fueling amount for obtaining the necessary torque to obtain the requested velocity. The EMS also assures that no oscillations arise in the powertrain. It monitors the turbo pressure and limits the fueling in case a sufficient amount of air is not available for the combustion process. Hence, the achievable torque might be limited. There are several brake systems in a modern HDV, ranging from the weaker exhaust brake to the strong brake discs. The BMS receives a deceleration request and typically blends the brake power from the different systems depending on the magnitude of the requested signal. It also assures that no system overheats. Therefore, the achieved braking force varies with respect to the current state of the system. The GMS is an automated gear changing system that enables the driver to devote more attention to handling the vehicle and to traffic. Monitoring the RPM and the engine torque request, it is designed to change the gear quickly and comfortably in a fuel-efficient manner. Note, however, that a delay typically arises when disengaging and engaging a new gear.

3. Modeling

In this section we present the models that serve as the basis for the controller structure presented in Section 4. First a brief description is given on the internal and external forces affecting a vehicle in motion. The longitudinal model is then extended to describe the dynamics of an HDV platoon. Finally, we present the performance criteria that are desirable for an HDV platoon. In Alam et al. (2011), performance criteria were presented for considering one preceding vehicle in the platoon. Here, we extend the criteria to include an arbitrary number of preceding vehicles. More details on the vehicle model, the characteristic coefficients, and its derivation can be found in Alam (2014).

3.1. Vehicle model

External forces are imposed on the vehicle. The external forces mainly consist of rolling resistance F^{r}, gravitational force F^{g}, and air drag F^{a}. The rolling resistance occurs due to the resistive frictional force that occurs between the road surface and the wheels. It is given by $F^{\mathrm{r}} = c_{\mathrm{r}} mg\cos\alpha$, where c_{r} denotes the roll resistance coefficient, g the gravitational constant, m the vehicle mass, and α the road grade. The gravitational force, $F^{\mathrm{g}} = mg\sin\alpha$, can act as a positive or a negative longitudinal force depending on the incline of the road. The aerodynamic drag has a strong impact on an HDV and can amount up to 50% of the total resistive forces at full speed. It is given by $F^{\mathrm{a}} = \frac{1}{2} c_{\mathrm{w}} \Phi(d) A \rho v^2$, where A denotes the maximum cross-sectional area of the vehicle, ρ the air density, c_{w} the air drag coefficient, d the relative distance to a preceding vehicle, v the vehicle velocity, and $0.3 < \Phi(d) = k_{pw} d + l_{pw} \leq 1$ denotes the empirically derived air drag reduction due to the preceding vehicle. The parameters $k_{pw} < 0$ and $l_{pw} > 0$ are empirically derived Alam (2011, Chapter 3). A single HDV experiences an increased air pressure at the front of the vehicle and a pressure drop at the tail. This pressure change produces the aerodynamic drag inflicted upon the vehicle. The pressure is significantly reduced for a follower vehicle, operating at 50 m or less, since the preceding vehicle reduces the air flow inflicted upon its frontal surface, inducing a physical coupling between the vehicles. The preceding vehicle also experiences a small air drag reduction at very short inter-vehicle spacings. However, it can be neglected for the purpose of this study. Hence, we assume that $\Phi(d) = 1$ for the lead vehicle.

Let $i = 1, \ldots, N$ denote the vehicle order in the platoon. Applying Newton's second law of motion along with all the external forces described above, a non-linear vehicle model is derived as

$$\begin{aligned}
\dot{s}_i &= v_i \\
\dot{d}_{i-1,i} &= v_{i-1} - v_i \\
m_t \dot{v}_i &= F_i^{\mathrm{e}} - F_i^{\mathrm{b}} - F_i^{\mathrm{a}}(v_i, d_{i-1,i}) - F_i^{\mathrm{r}}(\alpha(s_i)) - F_i^{\mathrm{g}}(\alpha(s_i)) \\
&= k_i^{\mathrm{e}} T_i^{\mathrm{e}}(\omega_i, \delta_i) - F_i^{\mathrm{b}} - k_i^{\mathrm{d}} \Phi(d_{i-1,i}) v_i^2 - k_i^{\mathrm{r}} \cos\alpha(s_i) - k_i^{\mathrm{g}} \sin\alpha(s_i) \qquad (1)
\end{aligned}$$

where s_i is the absolute traveled distance for HDV i from a reference point common to all vehicles in the platoon, $d_{i-1,i}$ denotes the relative distance between vehicle $i-1$ and i, v_i is the velocity, $\alpha(s_i)$ denotes the road grade at point s_i on the road, m_{t_i} is the total inertial mass, $F_i^{\mathrm{e}} \geq 0$ denotes the force produced by the engine through fuel injection, $F_i^{\mathrm{b}} \geq 0$ denotes the braking force, and k_i^l, $l \in \{\mathrm{e}, \mathrm{d}, \mathrm{r}, \mathrm{g}\}$, are characteristic coefficients. The control input T_i^{e} is the net engine torque, which is a function of the engine angular velocity ω_i and the injected fuel amount δ_i. It is determined by the EMS, which receives a velocity request as an input. Furthermore, the control input F_i^{b} is determined through the BMS, which receives an acceleration demand as an input. The EMS determines the required fuel injection to produce the necessary propulsion torque for achieving the velocity input to the system. Similarly, the separate BMS determines the required force that needs to be generated to obtain the acceleration input to the system. Hence, two system dynamics models are required for the different modes of operation. To account for the additional system dynamics produced by the EMS in the vehicles under consideration, for simplicity, its computed control input can be modeled as

$$T_{e_i}(t) = K_i^{\mathrm{c}} \left(e_i(t) + \frac{1}{T_i^{\mathrm{I}}} \int_0^t e_i(\theta)\, d\theta \right), \qquad (2)$$

where $e_i = v_i^{\mathrm{ref}} - v_i$ and K_i^{c}, T_i^{I} are design parameters obtained and set according to the engine specifications. By inserting the model for the EMS into (1), the nonlinear system model for a single HDV in a platoon is given as

$$\begin{aligned}
m_{t_i} \dot{v}_i &= k_i^{\mathrm{e}} K_i^{\mathrm{c}} \left(e_i + \frac{1}{T_i^{\mathrm{I}}} \int e_i\, dt \right) - k_i^{\mathrm{d}} \Phi(d_{i-1,i}) v_i^2 - k_i^{\mathrm{r}} \cos\alpha_i - k_i^{\mathrm{g}} \sin\alpha_i \\
&= k_i^{\mathrm{e}} K_i^{\mathrm{c}} v_i^{\mathrm{ref}} - k_i^{\mathrm{e}} K_i^{\mathrm{c}} v + z_i^{\mathrm{v}} - k_i^{\mathrm{d}} \Phi(d_{i-1,i}) v^2 - k_i^{\mathrm{r}} \cos\alpha_i - k_i^{\mathrm{g}} \sin\alpha_i, \\
\dot{z}_i^{\mathrm{v}} &= \frac{k_i^{\mathrm{e}} K_i^{\mathrm{c}}}{T_i^{\mathrm{I}}} e_i \qquad (3)
\end{aligned}$$

where v_i^{ref} is the control input to the EMS and z_i^{v} is an integral state in the EMS model. The vehicle dynamics with the BMS is significantly faster, since a relatively large deceleration force can be produced by the brake system. Thus, it is assumed that the input to the BMS is obtained instantaneously, hence the nonlinear system model during braking is given as

$$m_{t_i} \dot{v}_i = m a_i^{\mathrm{ref}} - k_i^{\mathrm{d}} \Phi(d_{i-1,i}) v_i^2 - k_i^{\mathrm{r}} \cos\alpha_i - k_i^{\mathrm{g}} \sin\alpha_i \qquad (4)$$

where a_i^{ref} is the input signal to the BMS.

3.2. Platoon model

Here, we develop a model to capture the platoon dynamics. We first introduce the state

$$z^{\mathrm{d}}_{i-1,i}(k+1) = z^{\mathrm{d}}_{i-1,i}(k) + T_s(d_{i-1,i}(k) - \tau v_i(k)), \tag{5}$$

as the integral action for maintaining the time headway policy, where T_s is the sampling time, and τ is the time headway constant. Let the state vector be partitioned as

$$x = [\underbrace{z^{\mathrm{v}}_1\ v_1}_{x_1}\ \ \underbrace{d_{12}z^{\mathrm{d}}_{12}\ z^{\mathrm{v}}_2\ v_2}_{x_2}\ \ \underbrace{d_{23}z^{\mathrm{d}}_{23}z^{\mathrm{v}}_3\ v_3}_{x_3}\ \ \dots\ \ \underbrace{d_{N-1,N}z^{\mathrm{d}}_{N-1,N}z^{\mathrm{v}}_N v_N}_{x_N}]^T. \tag{6}$$

Then, a discrete linearized state space representation of the system can be given as

$$x(k+1) = \underbrace{\begin{bmatrix} A_{11} & 0 & 0 & \dots & 0 \\ A_{21} & A_{22} & 0 & \dots & 0 \\ 0 & A_{32} & A_{33} & \dots & 0 \\ \vdots & \vdots & \vdots & \ddots & \vdots \\ 0 & 0 & 0 & \dots & A_{NN} \end{bmatrix}}_{A} \underbrace{\begin{bmatrix} x_1(k) \\ x_2(k) \\ x_3(k) \\ \vdots \\ x_N(k) \end{bmatrix}}_{x(k)} + \underbrace{\begin{bmatrix} B_1 & 0 & 0 & \dots & 0 \\ 0 & B_2 & 0 & \dots & 0 \\ 0 & 0 & B_3 & \dots & 0 \\ \vdots & \vdots & \vdots & \ddots & \vdots \\ 0 & 0 & 0 & \dots & B_N \end{bmatrix}}_{B} \underbrace{\begin{bmatrix} u_1(k) \\ u_2(k) \\ u_3(k) \\ \vdots \\ u_N(k) \end{bmatrix}}_{u(k)}, \tag{7}$$

which is sampled with $T_s = 0.01$ s. The system matrices A and B follow immediately from discretizing and linearizing (1), (3), and (4) with respect to a reference velocity, an engine torque which maintains the velocity, a fixed time headway between the vehicles, and a constant road grade. For simplicity we assume that the road grade is constant due to lack of road topography preview information (Sahlholm & Johansson, 2010).

3.3. Performance criteria

The performance criteria for the HDV platoon can be formulated into a quadratic cost, by imposing costs on deviating in relative velocity, spacing, and the control effort. Hence, we formulate the weight parameters for a quadratic cost function based upon performance and safety objectives. The overall objective of the vehicles traveling in a platoon is to reduce the fuel consumption, while maintaining a desired inter-vehicle spacing. Let $\mathcal{N}_i = [i-n_i, \dots, i-1]$ denote the set of n_i preceding vehicles that are within radio range of vehicle i and let $x_{\mathcal{N}_i}$ denote their corresponding states. Hence, the cost for each local subsystem in the HDV platoon can be set up as

$$\begin{aligned} J_i(u_i) &= \sum_{k=0}^{\infty} \left(\sum_{\forall j \in \mathcal{N}_i} w^{\tau}_j (z^{\mathrm{d}}_{ji}(k))^2 + w^{v}_{ji}(v_j(k) - v_i(k))^2 + w^{u}_i (u_i(k))^2 \right) \\ &= \sum_{k=0}^{\infty} \left(\begin{bmatrix} x_{\mathcal{N}_i}(k) \\ x_i(k) \end{bmatrix}^T Q_i \begin{bmatrix} x_{\mathcal{N}_i}(k) \\ x_i(k) \end{bmatrix} + R_i (u_i(k))^2 \right) \end{aligned} \tag{8}$$

where the dimension of Q_i varies with the number of vehicles within radio range and can be chosen differently for the vehicle controllers. $R_i = w^{u}_i$ is the control input weight, which is directly proportional to the vehicle propulsion or braking energy.

The weights give a direct interpretation of how to enforce the objectives for a vehicle traveling in a platoon. The value of w^{v}_{ji} sets a cost for deviating from the velocity of the preceding vehicles. The magnitude of w^{τ}_i determines the importance of not deviating from the desired time headway setting. Hence, a large w^{τ}_i puts emphasis on safety. If w^{τ}_i and w^{v}_{ji} are large, the control input creates an overshoot if the preceding vehicles deviate from the current velocity, since the controller mandates a quick compensation. Similarly, the controller is also sensitive to small disturbances in the preceding vehicles' behavior with large w^{τ}_i and w^{v}_{ji}. On the other hand, an overshoot also occurs if the weights are small, since a soft control allows for large initial deviation from the reference for inter-vehicle spacing, which must be compensated by catching up with a higher velocity. Hence, there is a trade-off in disturbance rejection and performance, when determining the weights. Finally, w^{u}_i punishes the control effort which is proportional to the fuel consumption. Since the performance criteria for the platoon can be formulated as the quadratic cost in (8), the infinite horizon LQR is a suitable controller with small memory usage. Furthermore, since the Riccati solution for the infinite horizon LQR needs only to be computed once, as opposed to the finite horizon LQR, the computational complexity is also reduced.

To choose the weights in (8), some engineering intuition is needed. One suggestion is to choose the weights such that the closed-loop system satisfies a condition on that disturbances should be attenuated between two neighboring vehicles. The l_2-condition, a common criterion for string stability (Swaroop, 1994), can be used as a reference for obtaining a desirable platooning behavior. In Alam et al. (2011) we showed how to select the weights in (8) to achieve string stability for a homogeneous platoon and in Alam (2014) it was shown for a heterogeneous platoon.

4. Control design

In this section we present a method for deriving the decentralized controllers for an arbitrary number of preceding vehicles. The proposed controller is shown in detail in Fig. 4. Finally a simple bumpless transfer scheme, based on performance and driver acceptance, is given for switching between the low-level EMS and BMS controllers.

4.1. Suboptimal platooning controller

The system state vector for deriving the control law when the vehicles are operated with the EMS is given by (6) and the control

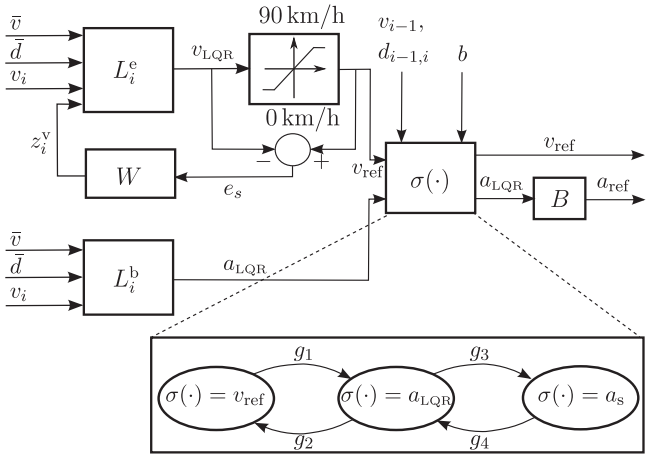

Fig. 4. Overview of the proposed LQR with bumpless transfer. The velocity information from all the preceding vehicles is denoted by $\bar{v}$ and the inter-vehicle spacing information is denoted by $\bar{d}$. Velocity measured from the on-board sensors of the vehicle is denoted by v_i. The velocity as well as the distance measured from the preceding vehicle is denoted by v_{i-1} and $d_{i-1,i}$, respectively. z^{v}_i denotes the integral state in the EMS model.

input is then given by $u^e = [v_1^{ref}\ v_2^{ref}\ v_3^{ref}\ \dots\ v_N^{ref}]^T$. However, the state vector for deriving the control law during braking is chosen as a subset of (6):

$$x^b = [\underbrace{v_1}_{x_1^b}\ \underbrace{d_{12}v_2}_{x_2^b}\ \underbrace{d_{23}v_3}_{x_3^b}\ \dots\ \underbrace{d_{N-1,N}v_N}_{x_N^b}]^T,$$

and the corresponding control input for the system is $u^b = [a_1^{ref}\ a_2^{ref}\ a_3^{ref}\ \cdots\ a_N^{ref}]^T$. The integral state is omitted in the system model for the brake control law, mainly to remove the damping in the system that follows from having $z_{i-1,i}^d$ in the feedback. By removing the state, the controller will try to maintain the larger equilibrium distance during a braking event, which is experienced as more safe and intuitive by the expert drivers that evaluated the system. The system matrices for when the vehicles are governed by the engine are denoted by A^e and B^e. The system matrices for when the vehicles are governed by the brakes are denoted by A^b and B^b, with rows and columns of (7) removed according to the definition of x^b. Note that A^q and B^q, $q \in \{e, b\}$, are lower triangular band matrices. However, elements differ between the two modes of operation.

The particular structure of the system (7) can be divided into subsystems. Thereby, as presented in Algorithm 1, locally stabilizing controllers can be derived sequentially by starting from the lead vehicle and then transmitting the controller gain and subsystem parameters, along with the state information to all the follower vehicles. As a result of subsequently deriving controllers based on local model information and interconnections, a global suboptimal decentralized feedback control law, $u^q(k) = -L^q x^q(k)$, is produced with respect to (7), where L has a lower block diagonal form and is given as

$$L = \begin{bmatrix} L_{11}^q & 0 & 0 & \dots & 0 \\ L_{21}^q & L_{22}^q & 0 & \dots & 0 \\ L_{31}^q & L_{32}^q & L_{33}^q & \dots & 0 \\ \vdots & \vdots & \vdots & \ddots & \vdots \\ L_{N1}^q & L_{N2}^q & L_{N3}^q & \dots & L_{NN}^q \end{bmatrix}. \tag{9}$$

Note that the feedback gain matrix in (9) is given in a general form. However, it can have a lower band diagonal structure depending on the radio range. When the communication range is limited, the states for the first or other preceding vehicles outside the range cannot be considered and the corresponding matrix elements in (9) are then zero. The decentralized optimization is performed for each subsystem, as described in Algorithm 1, where it is assumed that each subsystem is stabilizable and detectable. The controllers can then be derived as

Algorithm 1.

Step (0) Set the weight matrices Q_i^q, R_i^q, $i = 1, \dots, N$, to be positive definite and in accordance with the desired performance criteria. It is assumed that the pairs $(\overline{A}_{ii}^q, \overline{B}_i^q)$ and $(\overline{Q}_i^q, \overline{A}_{ii}^q)$, given in the algorithm, are stabilizable and detectable, respectively.

Step (1) Compute the optimal feedback controller, u_1^{q*}, for vehicle 1 (the lead vehicle) by solving

$$\min_{u_1} \sum_{k=0}^{\infty} x_1^q(k)^T Q_1^q x_1^q(k) + u_1^q(k)^T R_1^q u_1^q(k)$$
$$\text{s.t.}\quad x_1^q(k+1) = A_{11}^q x_1^q(k) + B_1^q u_1^q(k).$$

The optimal linear quadratic feedback controller is then given by

$$u_1^{q*}(k) = -L_1^q x_1^q(k),$$
$$L_1^q = (R_1^q + B_1^{qT} P_1^q B_1^q)^{-1} B_1^{qT} P_1^q A_1^q,$$

where P_1^q is the unique positive definite solution of

$$P_1^q = A_{11}^{qT}(P_1^q - P_1^q B_1^q (R_1^q + B_1^{qT} P_1^q B_1^q)^{-1} B_1^{qT} P_1^q) A_1^q + Q_1^q.$$

Step (2) Compute the optimal feedback controllers, u_i^{q*}, for vehicles $i = 2, \dots, N$,

$$\min_{u_i} \sum_{k=0}^{\infty} \begin{bmatrix} x_{\mathcal{N}_i}^q(k) \\ x_i^q(k) \end{bmatrix}^T Q_i^q \begin{bmatrix} x_{\mathcal{N}_i}^q(k) \\ x_i^q(k) \end{bmatrix} + u_i^q(k)^T R_i^q u_i^q(k)$$

s. t.

$$\begin{bmatrix} x_{\mathcal{N}_i}^q(k+1) \\ x_i^q(k+1) \end{bmatrix} = \underbrace{\begin{bmatrix} A_{\mathcal{N}_i\mathcal{N}_i}^q - B_{\mathcal{N}_i}^q L_{\mathcal{N}_i}^q & 0 \\ A_{\mathcal{N}_i i}^q & A_{ii}^q \end{bmatrix}}_{\overline{A}_{ii}^q} \begin{bmatrix} x_{\mathcal{N}_i}^q(k) \\ x_i^q(k) \end{bmatrix} + \underbrace{\begin{bmatrix} 0 \\ B_i^q \end{bmatrix}}_{\overline{B}_i^q} u_i^q(k).$$

Obtain optimal u_i^{q*} by solving

$$u_i^{q*}(k) = -L_i^q \begin{bmatrix} x_{\mathcal{N}_i}^q(k) \\ x_i^q(k) \end{bmatrix},$$
$$L_i^q = (R_i^q + \overline{B}_i^{qT} P_i^q \overline{B}_i^q)^{-1} \overline{B}_i^{qT} P_i^q \overline{A}_{ii}^q,$$

where P_i^q is the unique positive definite solution of

$$P_i^q = \overline{A}_{ii}^{qT}(P_i^q - P_i^q \overline{B}_i^q (R_i^q + \overline{B}_i^{qT} P_i^q \overline{B}_i^q)^{-1} \overline{B}_i^{qT} P_i^q) \overline{A}_{ii}^q + Q_i^q.$$

The proof for that Algorithm 1 produces a globally asymptotically stable controller given in Alam (2014). Furthermore, even though the spacing states, $d_{i-1,i}$, between preceding vehicles are not controllable for an HDV downstream, an LQR solution can still be found since it is only required that each vehicle subsystem in Algorithm 1 is stabilizable and detectable. Another advantage of the proposed algorithm is that it is scalable. If a new vehicle would like to join the platoon at the tail, the decentralized platooning controllers do not need to be recomputed. Only the joining HDV needs to receive information regarding the parameters, control gains, and states from all the vehicles within communication range.

4.2. Bumpless switching

The objective for introducing bumpless transfer, in addition, is to avoid overshoots, uncomfortable behavior, or even hardware damage, when switching between actuation with the EMS and BMS. When one controller is active, the other inactive controller produces a control signal that might be different. For example, a large velocity might be requested after braking, which will mandate a high torque and the driver will experience a jerk. Excessive strain is then put on the powertrain components. Hence, it is essential to avoid switching transients. A rather standard method is followed to do bumpless transfer as discussed next (Åström & Hägglund, 2006).

It is not fuel efficient to brake, since the energy produced through diesel combustion is wasted through heat loss produced by the frictional forces in the brake discs. However, braking must be performed if the preceding vehicle decelerates by braking or the platooning HDVs are traversing a steep downhill segment without any preview information with respect to the upcoming topography (Alam, Mårtensson, & Johansson, 2013; Turri,

Besselink, Mårtensson, & Johansson, 2014). Therefore, we propose a control system that switches between engine and brake control, as illustrated in Fig. 4.

The feedback gain matrices L_i^e and L_i^b for the decentralized high-level controller, in Fig. 4, are established as given in Algorithm 1. A maximum velocity is enforced due to legislation on the speed demand to the EMS, which might saturate the control demand produced by the L_i^e. Hence, an anti-windup filter W is implemented as

$$z_i^v(k+1) = z_i^v(k) + \gamma_i T_s(e_i(k) + \frac{1}{T_t} e_s(k)) \tag{10}$$

where $\gamma_i = k_{e_i} K_i^c / m_{t_i} T_i^l$, $e_s = v_{\text{ref}} - v_{\text{LQR}}$, and T_t is a design parameter.

The switching guards, g_i in Fig. 4, between the three modes of operation are defined as

g_1 : $(d_{i-1,i} < \beta\tau v_i$ and $v_{i-1} < v_i)$ or $(b = 1$ and $d_{i-1,i} < \tau v_i)$;
g_2 : $d_{i-1,i} \geq \tau v_i$ and $v_{i-1} \geq v_i$ and $b = 0$ and $d_s < d_{i-1,i}$;
g_3 : $[v_i, d_{i-1,i}, v_r]^T \in \partial\mathcal{S}$;
g_4 : $[v_i, d_{i-1,i}, v_r]^T \in \mathcal{S}$;

where $b \in \{0, 1\}$ is a binary signal that is transmitted if a preceding vehicle brakes, d_s, is a minimum allowed spacing for safety, and $\beta \in [0, 1]$ is a design parameter that determines how much spacing is allowed to decrease from the reference spacing before the brakes should be applied. $\mathcal{S} = [0, v_i^{\max}] \times [d_{i-1,i}^{\min}, \infty] \times [v_r^{\min}, v_r^{\max}]$ denotes a safe set, derived through a game theoretical formulation for guaranteeing safety in HDV platooning (Alam et al., 2014), where v_r is the relative velocity with respect to the preceding vehicle. A collision can always be avoided despite the worst case behavior of the preceding vehicle if the vehicle states are inside the safe set, otherwise, a collision can occur. Hence, if a vehicle reaches the boundary of the safe set, denoted as $\partial\mathcal{S}$, an optimal collision avoidance brake request, a_s, is sent to the BMS to guarantee safety with the proposed controller. The collision avoidance is aborted and the control is resumed once the vehicle reaches sufficiently inside the safe set. The controller output, v_{ref}, is directly fed through if the vehicle operates within the allowed inter-vehicle spacing. If the spacing decreases below the allowed limit and the preceding vehicle has not started to increase its velocity, or if any of the preceding vehicles brake, the controller output, a_{LQR}, is fed through until the preceding vehicles cease braking and the spacing is resumed.

If the spacing to the preceding vehicles decreases slightly, a reduced reference velocity is initially provided by the proposed controller to decelerate and the engine torque will drop to zero. A large jerk might occur when switching to braking, since the spacing is shorter than the reference. To facilitate a bumpless transfer when the controller switches to a_{ref}, a low pass filter, $B(z) = (1-p)/(z-p)$, is implemented after the switch, where $p \in [0, 1)$ is a design parameter for establishing the rise-time of the filter. When switching back to governing the vehicle through the EMS, v_{ref} should be close to the current vehicle velocity and the integral state, z^v, must be initiated accordingly to avoid a switching transient. The minimum cost to go given in the infinite horizon LQR derivation is given by $x_k^T P x_k$ (Åström, 1970). Thus, the following optimization problem can be set up to facilitate a bumpless transfer:

$$\min_{z_0^v} \quad \begin{bmatrix} \overline{x}_0 \\ z_0^v \end{bmatrix}^T \overline{P} \begin{bmatrix} \overline{x}_0 \\ z_0^v \end{bmatrix}, \quad \text{s.t.} \quad \|v_{\text{ref}} - v\|_\infty \leq \epsilon \tag{11}$$

where $\overline{x}_0$ are the known states and z_0^v is the initial integral state. The rearranged Riccati solution matrix is denoted as $\overline{P} = [\overline{P}_{11}\ \overline{P}_{12}; \overline{P}_{12}^T\ \overline{P}_{22}]$, where the columns and rows in P corresponding to z_0^v are shifted to match the state vector in (11). Finally, $\epsilon \geq 0$ is a design parameter that determines the level of smoothness in the transition. The solution to the optimization is given as

$$z_0^{v*} = \min\left(\max\left(\tilde{z}_0^v, \frac{-\epsilon - L_x\overline{x}_0 - v}{L_z}\right), \frac{\epsilon - L_x\overline{x}_0 - v}{L_z}\right), \tag{12}$$

where we have used the fact that $v_{\text{ref}} = -Lx_0 = -L_x\overline{x}_0 - L_z z_0^v$ and that $\tilde{z}_0^v = -2\overline{P}_{22}^{-1}\overline{P}_{12}^T\overline{x}_0$ is the solution to minimizing the quadratic cost in (11). Note that if $\epsilon = 0$, the quadratic cost is neglected and a seamless transfer is obtained.

5. Numerical evaluations

Numerical evaluations for a three-HDV platoon are presented in this section for typical highway scenarios. The scenarios are carried out by feeding an automated velocity or deceleration reference to the lead vehicle. An advanced simulation model, see Alam (2011, Chapter 3), is used to tune the weight parameters, Q_i^q and R_i^q, in the LQR cost formulation (8) and to evaluate the performance of the platooning vehicles. The simulation model consists of 3313 variables, 1058 equations, and 626 states for each vehicle, where each of the components in the powertrain is modeled carefully and verified to mimic real life behavior for a single HDV. The vehicle configuration and parameters in the given simulations are set with respect to the real vehicles that are used for a qualitative verification of the obtained results, as presented in Section 6. The time headway constant is set to $\tau = 1$ s, which is typically the smallest ACC setting in modern vehicles. Even though the behavior of the simulation model is verified for a single vehicle, it might not capture all the dynamics of a real vehicle platoon. Hence, we validate the results presented in this section through empirical findings for a three-HDV platoon in Section 6.

5.1. Acceleration responses

Several step responses of varying step sizes were simulated to evaluate the proposed controller. In Fig. 5, simulation results are given for a scenario when the lead vehicle initially drives at a low velocity of 50 km/h. After reaching steady state, the lead vehicle increases its velocity by 10 km/h, then maintains the new set velocity for 35 s and then performs an additional step of 10 km/h. The top plot in Fig. 5 shows the velocity trajectories for the platooning vehicles, where the indices denote the vehicle position index in the platoon. The second from top plot shows the relative distances between the vehicles, the second from bottom plot shows the error in relative distance given as the deviation from the set time headway policy:

$$e_{i-1,i} = d_{i-1,i} - \tau v_i, \tag{13}$$

and the bottom plot shows the corresponding acceleration trajectories for all the vehicles. The results show that the overshoot in the velocity and relative distance is lower for the last vehicle compared to the vehicle in the middle of the platoon. The lead vehicle has an overshoot[1] in velocity of 6% during the first step response and an overshoot of 5% during the second step response. The second vehicle has corresponding overshoots of 14% and 17%. The third vehicle has an overshoot of 12% and 17%, respectively. Hence, the overshoot is only dampened in the first step response. The attenuation is lost during the second step response because a gear change is made in the last vehicle during the step, which the two preceding vehicles deter until the steady state is resumed. The deviation from the reference for inter-vehicle spacing is always smaller for the third vehicle during the steps. The sign of the

[1] The overshoot is given by the maximum deviation from the velocity increase divided by the velocity increase magnitude.

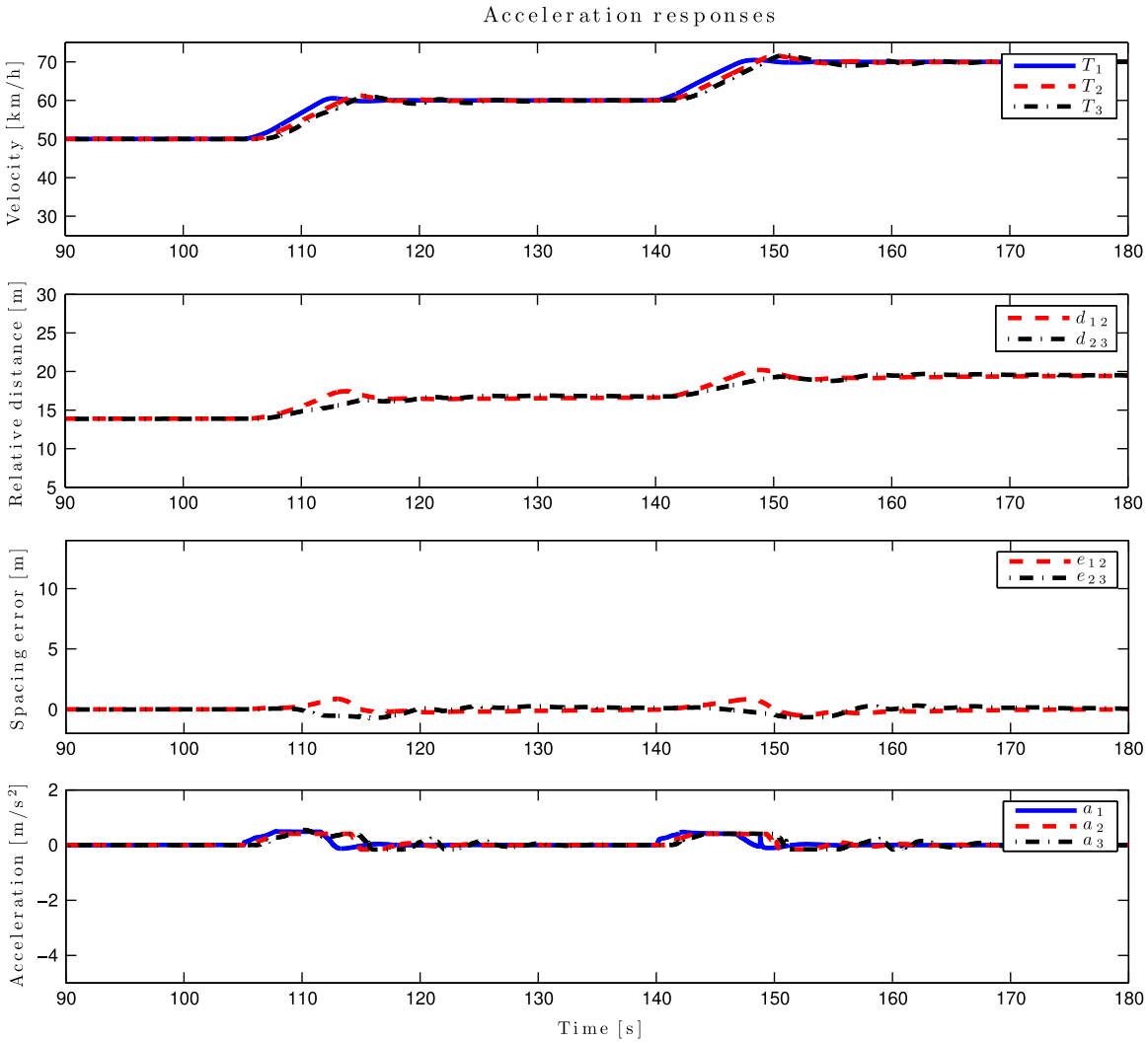

Fig. 5. Simulated step responses when the first vehicle in the platoon increases its velocity by 10 km/h. The solid (blue) lines are the trajectories for the lead vehicle, the (red) dashed lines are the trajectories for the vehicle in the middle, and the (black) dashed-dotted lines are the trajectories for the last vehicle in the platoon. (For interpretation of the references to color in this figure caption, the reader is referred to the web version of this paper.)

deviation for the two follower vehicles is opposite because there is a slight lag in initiating the step for the second vehicle. However, the third vehicle experiences the same lag in response from the lead vehicle and considers the spacing error for all preceding vehicles. It can therefore handle the disturbance better. Furthermore, the propagated deviations from the reference for inter-vehicle spacing seem to stay bounded throughout the platoon.

5.2. *Braking responses*

To evaluate the transient responses of the distributed controller during and after braking, several simulations were carried out with varying external deceleration magnitude given to the first vehicle's automated controller. Fig. 6 displays the trajectories for when the first vehicle is given an external deceleration command of 3 m/s^2. After the vehicles reach a steady state velocity of 60 km/h, the braking is initiated until the lead vehicle has reduced its velocity by 10 km/h. The next braking is initiated after 18 s and the procedure is repeated until the lead vehicle has reached 30 km/h. It can be seen in the top plot of Fig. 6 that both follower vehicles have a bigger undershoot in velocity, compared to the first vehicle, after each braking has ended. The first vehicle has an undershoot in velocity of 16%, 25%, 6% during the first, the second, and the third step, respectively. The follower vehicles have corresponding undershoots in velocity of 19%, 40%, 19%. Thus, the follower vehicles have larger undershoots in velocity, but the third vehicle never displays a bigger undershoot than its preceding vehicle.

The spacing errors between the platooning vehicles, shown in the second from bottom plot, show that the controller in the third vehicle allows for a positive deviation from the reference for inter-vehicle spacing during deceleration. This is a consequence of the controller striving to compensate for the spacing error with respect to both preceding vehicles and not having the state $z^{\mathrm{d}}_{i-1,i}$ in the feedback control during braking. The desired time headway is later resumed after the braking is over. Because the braking event is transmitted through wireless communication, the second vehicle is also able to react very fast, only having a maximum deviation from the reference for inter-vehicle spacing of 0.6 m at most during the first braking. However, at the 130 s time marker, it can be seen that the second vehicle drops in velocity and requires some time to compensate for the increased deviation in spacing. This is due to the fact that a gear change at the moment the vehicle is about to resume the steady state velocity. Furthermore, the bottom plot in Fig. 6 shows that the deceleration is lower for the last vehicle at the cost of having to brake over a longer time period. However, the required braking power to handle the disturbance is lowered along the platoon and it can be inferred that the controller operates smoothly and safely.

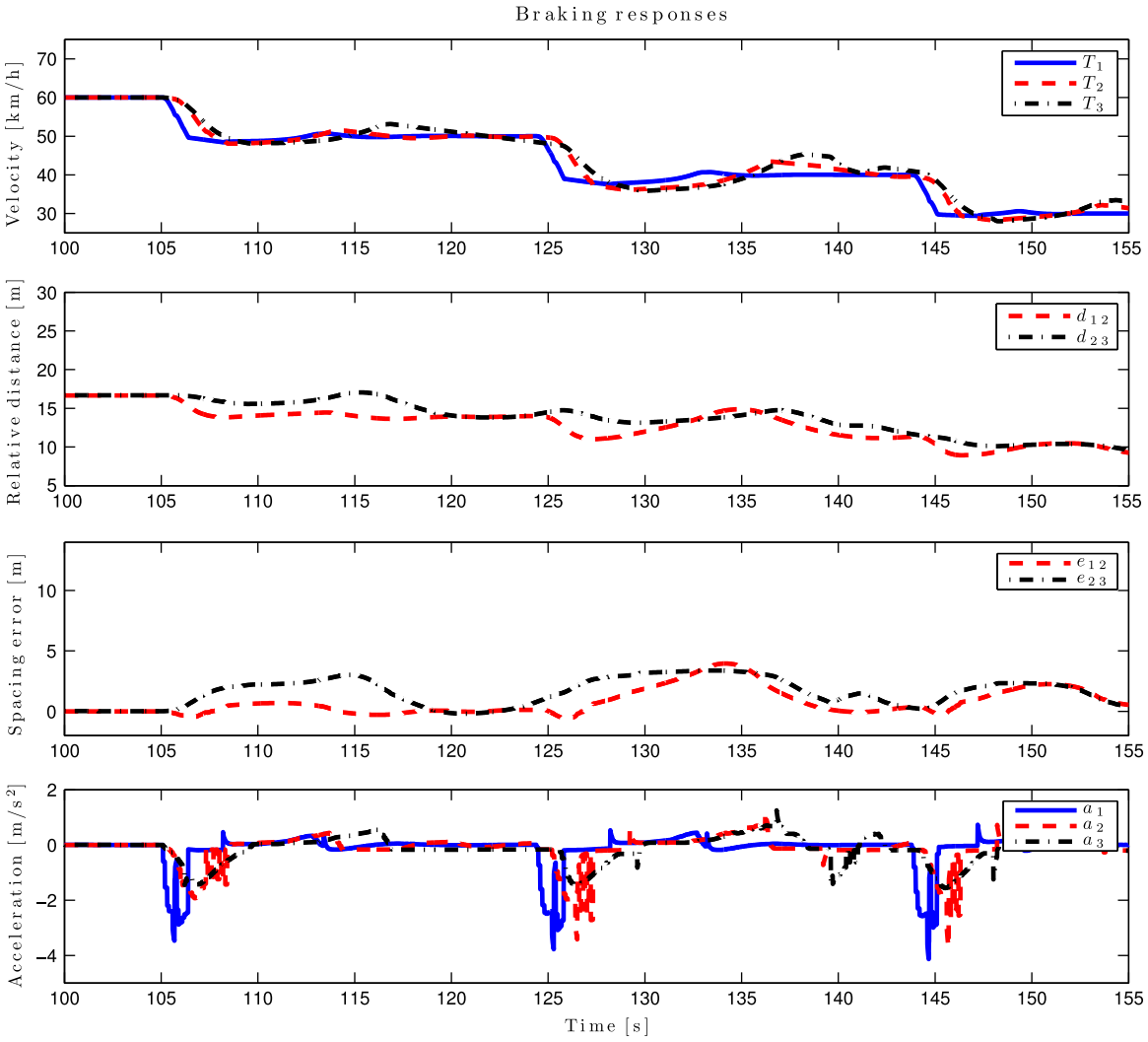

Fig. 6. Simulated responses when the first vehicle in the platoon decreases its velocity by 10 km/h through a deceleration of 3 m/s^2. The solid (blue) lines are the trajectories for the lead vehicle, the (red) dashed lines are the trajectories for the vehicle in the middle, and the (black) dashed-dotted lines are the trajectories for the last vehicle in the platoon. (For interpretation of the references to color in this figure caption, the reader is referred to the web version of this paper.)

5.3. *Alternating acceleration responses*

The goal of this scenario is to excite unmodeled dynamics in all the platooning vehicles and evaluate the controller performance when the control input is saturated. To this end, the first vehicle, starting from steady state, then accelerates with a given acceleration until it reaches an upper velocity limit. It then decelerates with a given deceleration demand until a lower velocity limit is reached. The alternating harsh accelerations and decelerations could be considered as analogous to behavior observed in a traffic queue that can occur on highways.

Fig. 7 shows the trajectories of the three platooning HDVs in one such scenario, where the first vehicle initially maintains 50 km/h and then starts to accelerate with 0.5 m/s^2 until it reaches the upper limit of 60 km/h. When the upper limit is reached, it then decelerates with 1 m/s^2 until it reaches the lower limit of 40 km/h, for when it again resumes the acceleration to the upper set speed. It can clearly be seen in the top plot of Fig. 7, between the 120 and 140 s time markers that the slope of the velocity changes during the acceleration. This occurs due to a gear change, during which an HDV can drop significantly in speed. The dynamics of the gear changes are not modeled and seem to occur at different times during the acceleration for all the vehicles depending on the current engine mode. The error in spacing, given in the second from bottom plot, shows that the deviation from the reference for inter-vehicle spacing grows initially for the last vehicle with the proposed control law, but remains limited. The second vehicle in the platoon maintains the spacing with a largest observed deviation of 2.8 m. The third vehicle has a larger observed deviation of 6.8 m, due to the significant drops in speed during each gear change, and then compensates for the inter-vehicle spacing error during the acceleration. The top plot with the velocity trajectories and the bottom plot with the vehicle acceleration trajectories show that there is no overshoot in velocity or acceleration. However, a gear change causes an increase in spacing due to the velocity drop until the new gear is engaged and full engine torque is regained.

6. Experimental evaluations

In this section, we first give the experimental setup for the three vehicle platoon. We then present empirical results for the three scenarios, presented in Section 5, that were obtained on a 1.7 km flight runway, south of Stockholm. The same automated control strategy was used to govern the first vehicle in the

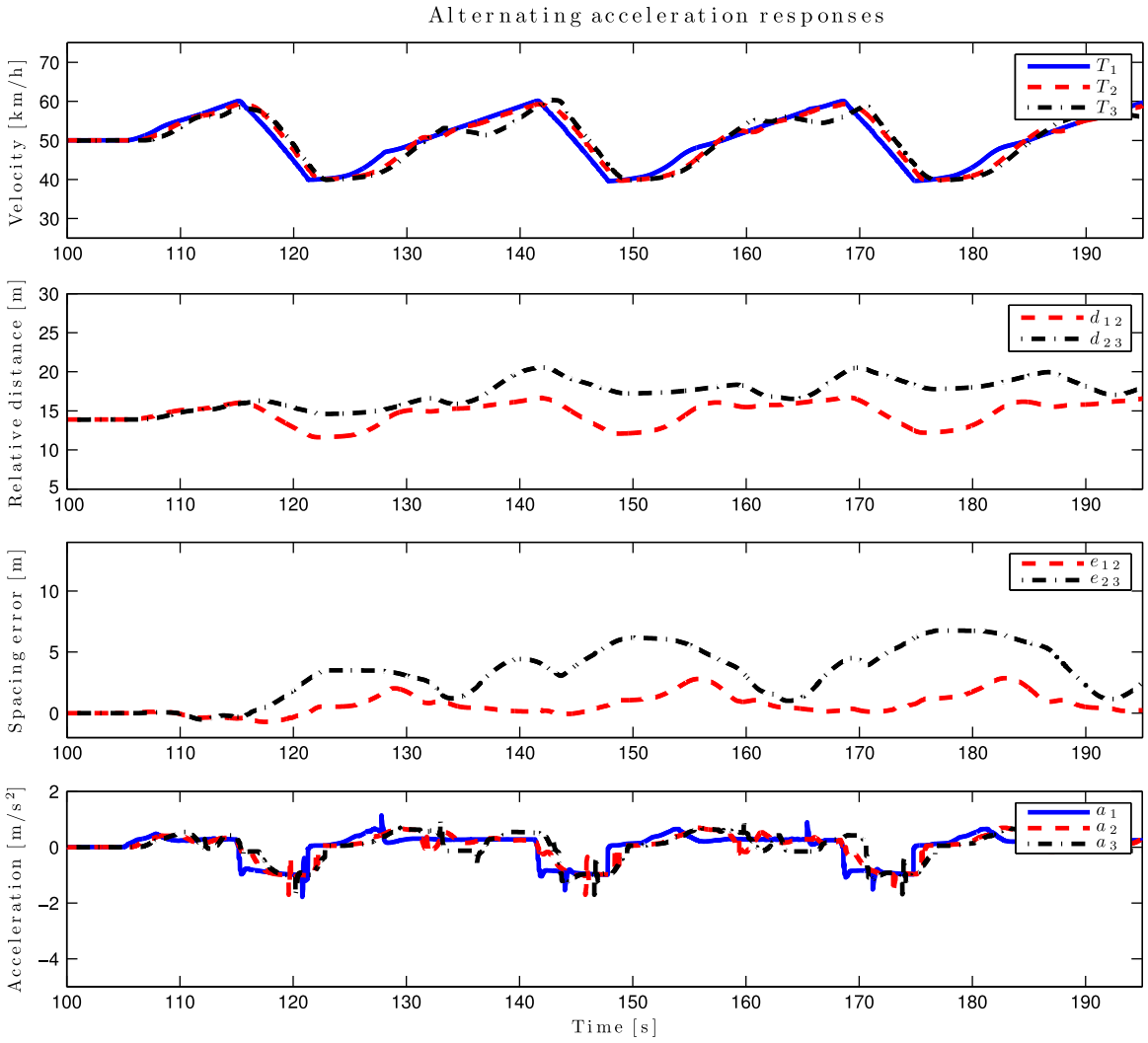

Fig. 7. Simulation to evaluate the controller performance when the lead vehicle varies its velocity. The solid (blue) lines are the trajectories for the lead vehicle, the (red) dashed lines are the trajectories for the vehicle in the middle, and the (black) dashed-dotted lines are the trajectories for the last vehicle in the platoon. (For interpretation of the references to color in this figure caption, the reader is referred to the web version of this paper.)

experiment procedure, in order to obtain reproducible results. Several experimental results are presented to evaluate the performance of the proposed controller in practice and evaluate the quality of the results from the simulation model.

6.1. Experimental setup

Three standard Scania tractor-trailer HDVs are utilized with additional control and communication hardware. All tractors have a 4×2 vehicle configuration and the trailers have three axles. The masses are measured to be $37.47t$ for the lead vehicle, $38.36t$ for the second vehicle, and $39.44t$ for the last vehicle in the platoon. They are equipped with a standard doppler radar, which sends the relative distance with a 40 ms interval to the central coordinator ECU and is gated every 100 ms. The final gear ratios are slightly different for each vehicle, with i_f=2.92 for the lead vehicle, i_f=2.71 for the second vehicle, and i_f=2.59 for the third vehicle. All vehicles are equipped with slightly different, but fully automatic gearboxes. Standard GPSs and ECUs, utilized in Scania HDVs, are used for positioning and executing the proposed controller, respectively. As illustrated in Fig. 8, a WSU carrying the standard wireless communication protocol 802.11p is mounted in each vehicle. The WSU is directly connected to the HDVs internal CAN system and messages are broadcast on

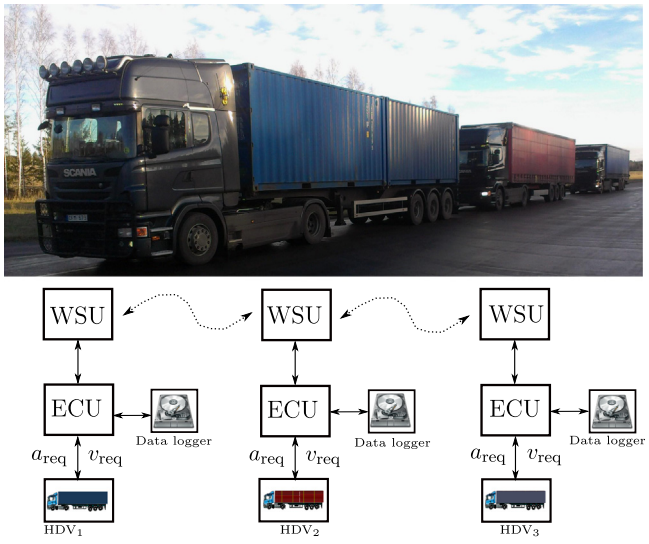

Fig. 8. A schematic overlay of the experimental hardware setup. The top picture shows the HDVs utilized in these experiments. The left HDV is the lead. The WSU, ECU, and data logger communicate through CAN. As soon as new information is obtained through the ECU or the vehicle, it is broadcast through the WSU.

demand. Thereby, the internal CAN signals such as velocity, acceleration, parameters, and control inputs are available to all the vehicles in range. The data are logged in all the vehicles.

6.2. Acceleration responses

Due to the relatively short distance of the runway, it was difficult to achieve steady state and at the same time has enough distance to perform two desired step responses. The results for two step responses in the lead vehicle of 10 km/h are given in Fig. 9, where the top plot shows the velocity trajectories for the three platooning HDVs. The second from top plot shows the inter-vehicle spacings and the second from bottom plot shows the deviation from the reference for inter-vehicle spacing, in which it can be seen that the vehicles had not yet been able to reach steady state at the beginning of the first step response. Finally, the bottom plot shows the vehicle acceleration trajectories. As shown in the second from bottom plot in Fig. 9, there is a deviation from the reference for inter-vehicle spacing of 1.1 m for the middle vehicle and a deviation of 2.4 m for the third vehicle, when the step is initiated. The first vehicle has an overshoot in velocity of 14% during the first step response and an overshoot of 8% during the second step response.

This is higher compared to the numerical results and is due to different CC logic in the first vehicle. However, the overshoots decrease in the second step, which is congruent with the simulation model. The second vehicle has corresponding overshoots in velocity of 24% and 8%, respectively, and the third vehicle has overshoots in velocity of 33% and 40%. The variation for the error in relative distance is also initially smaller for the third vehicle. Then, at the 118 s time marker, a gear change is performed in the third vehicle just before the step response, which causes the vehicle to fall behind thereby causing a large overshoot by catching up. A similar behavior is observed in the simulation model, with a less severe overshoot. The additional lag in handling the step response occurs because the last vehicle decelerates, i.e. coasts, just before the step is initiated. Hence, the turbo pressure is low, which limits the engine from outputting the desired torque until the turbo pressure is regained. Thus, the preceding vehicles manage to increase their velocities before the third vehicle can do so, causing a large overshoot to compensate for the increased errors in spacing and velocity.

6.3. Braking responses

The results obtained when the first vehicle, after reaching a steady state velocity of 60 km/h, brakes with 3 m/s^2 until the

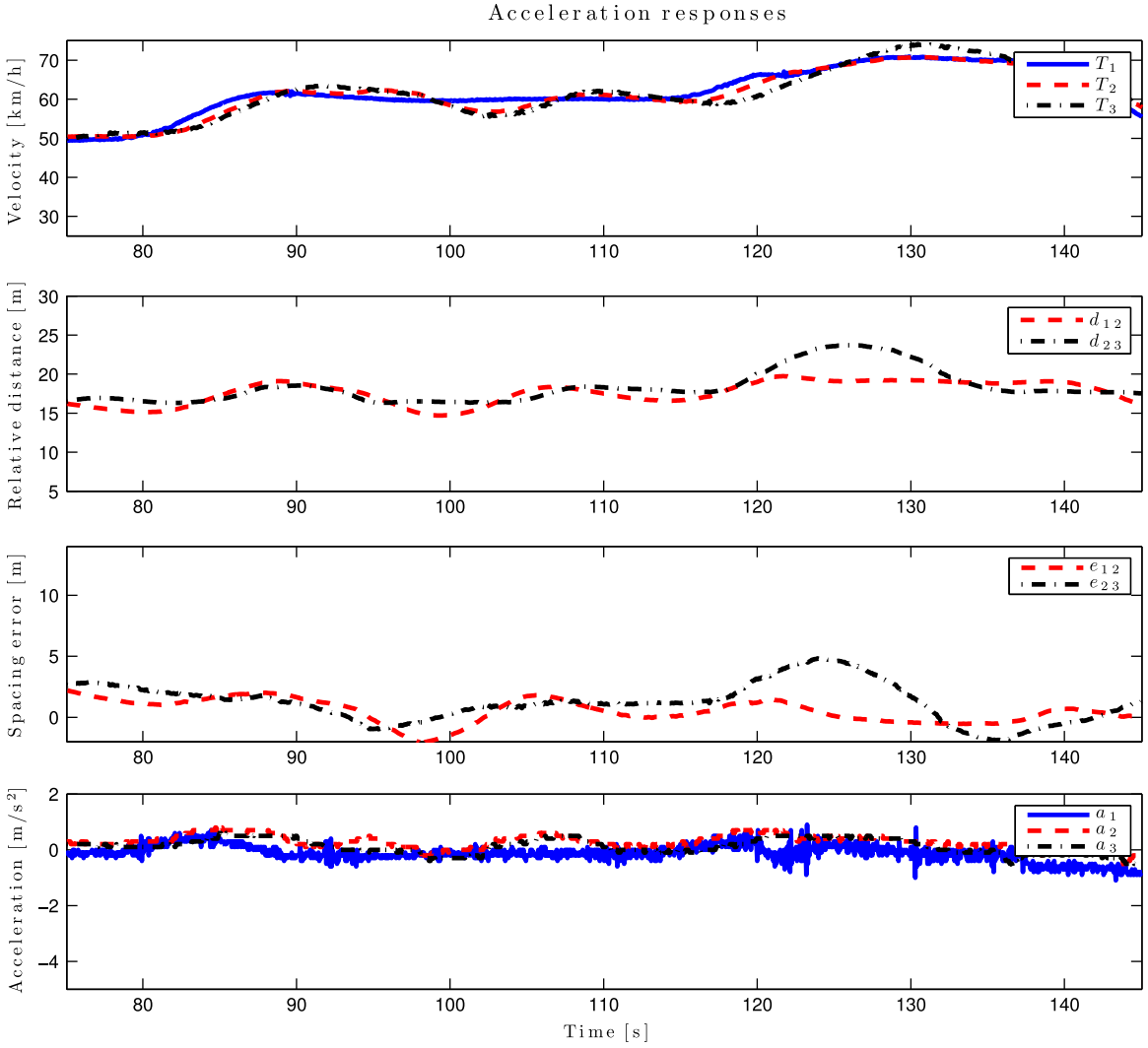

Fig. 9. Experiment results for step responses when the first vehicle in the platoon increases its velocity by 10 km/h. The solid (blue) lines are the trajectories for the lead vehicle, the (red) dashed lines are the trajectories for the vehicle in the middle, and the (black) dashed-dotted lines are the trajectories for the last vehicle in the platoon. (For interpretation of the references to color in this figure caption, the reader is referred to the web version of this paper.)

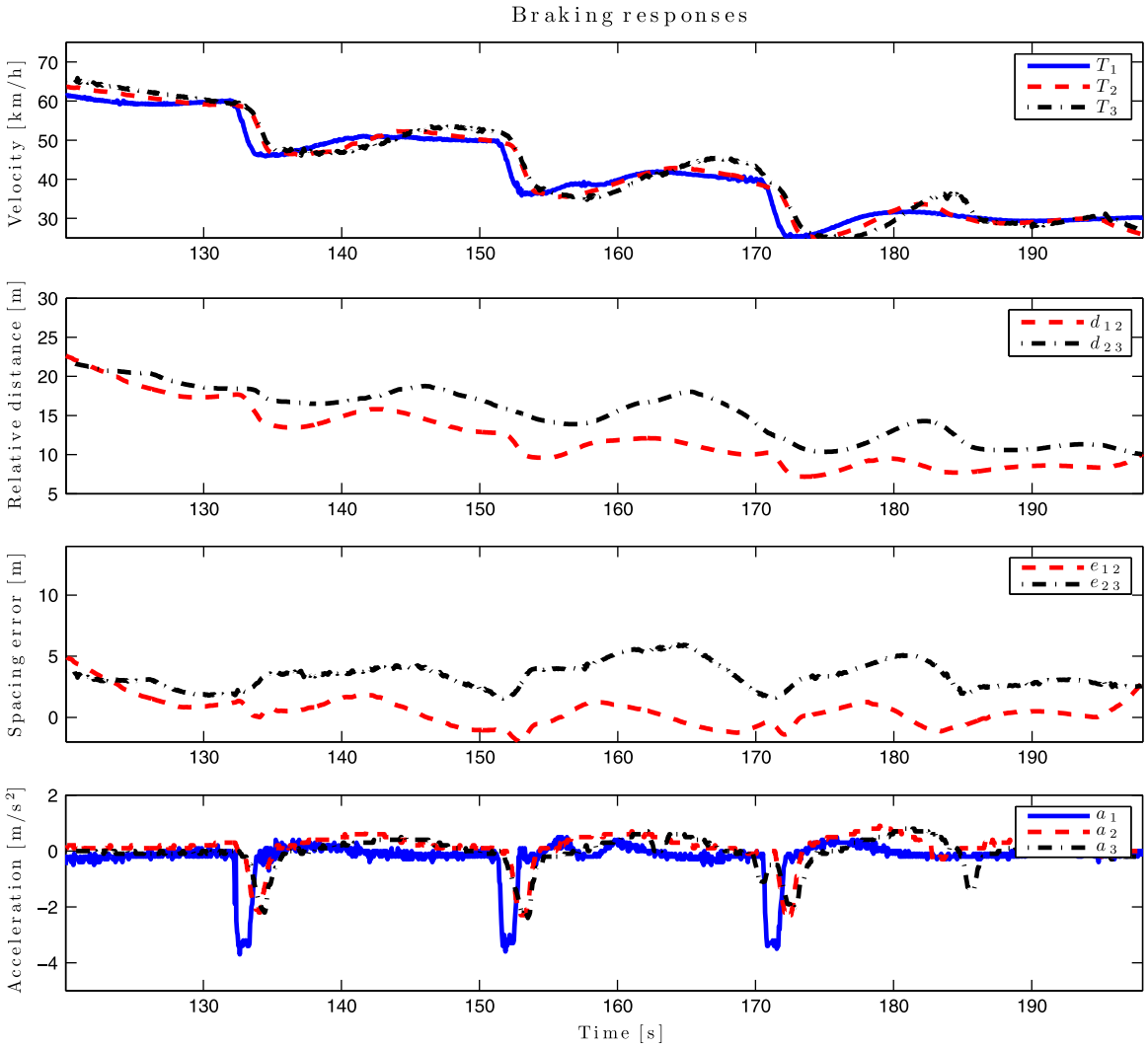

Fig. 10. Experiment results for when the first vehicle in the platoon decreases its velocity by 10 km/h through a deceleration of 3 m/s^2.

velocity is reduced by 10 km/h and then repeats the procedure after 18 s are given in Fig. 10. As can be seen in the second plot from the bottom, the vehicles had nearly reached steady state when the first braking is initiated, with an error in relative distance close to zero. The acceleration trajectories for all the vehicles, given in the bottom plot, show that the first vehicle performs the strongest deceleration, whereas the third vehicle has an equal or smaller deceleration compared to the second vehicle. The first vehicle has undershoots in velocity of 41% during the first two steps and 47% in the last. The follower vehicles both have undershoots in velocity of 37%, 45%, and 48%, respectively. Hence, the follower vehicles display a smaller undershoot during the first braking instance. In contrast to the simulation results, a severe overshoot in inter-vehicle spacing does not occur due to a gear change for the second vehicle. The third vehicle does not have a bigger undershoot than its preceding vehicle, which is congruent with the simulation model. The third vehicle maintains a larger relative distance, compared to the second vehicle, during the braking actions and then compensates for the error in relative distance after the braking is completed. A deviation from the reference for inter-vehicle spacing of -1.9 m occurs for the second vehicle, whereas the third vehicle always manages to maintain a positive deviation. After each braking event, when the proposed high-level controller switches back to the engine control, an unmodeled gear change occurs that results in an overshoot in desired inter-vehicle spacing. Nevertheless, the errors in relative distance stay limited. The controller performance is considered safe and the results are congruent with the simulation model.

6.4. Alternating acceleration responses

The results for the alternating accelerations and decelerations for the lead vehicle are given in Fig. 11. It can be seen that the maximum deviation from the reference for inter-vehicle spacing is 7.2 m for the last vehicle, which is nearly the same in the simulation model. However, the maximum error is larger for the second vehicle in contrast to the simulation results. This is due to a difference in gear management logic between the real vehicles and the simulation model. A periodic behavior can be observed in the plot for the relative distances and in the plot for the error in relative distance. The top plot in Fig. 11, for the velocity trajectories, reveals that a gear change occurs every other time an acceleration is performed, for the second vehicle, since there is a significant drop in velocity around the 105 s and 155 s time markers. The gear change results in a velocity decrease that creates an increase in relative distance. The second vehicle then manages to reduce the error in relative distance during the next acceleration phase. When the desired time headway is recovered, the behavior is repeated. Nevertheless, it can be seen that the spacing

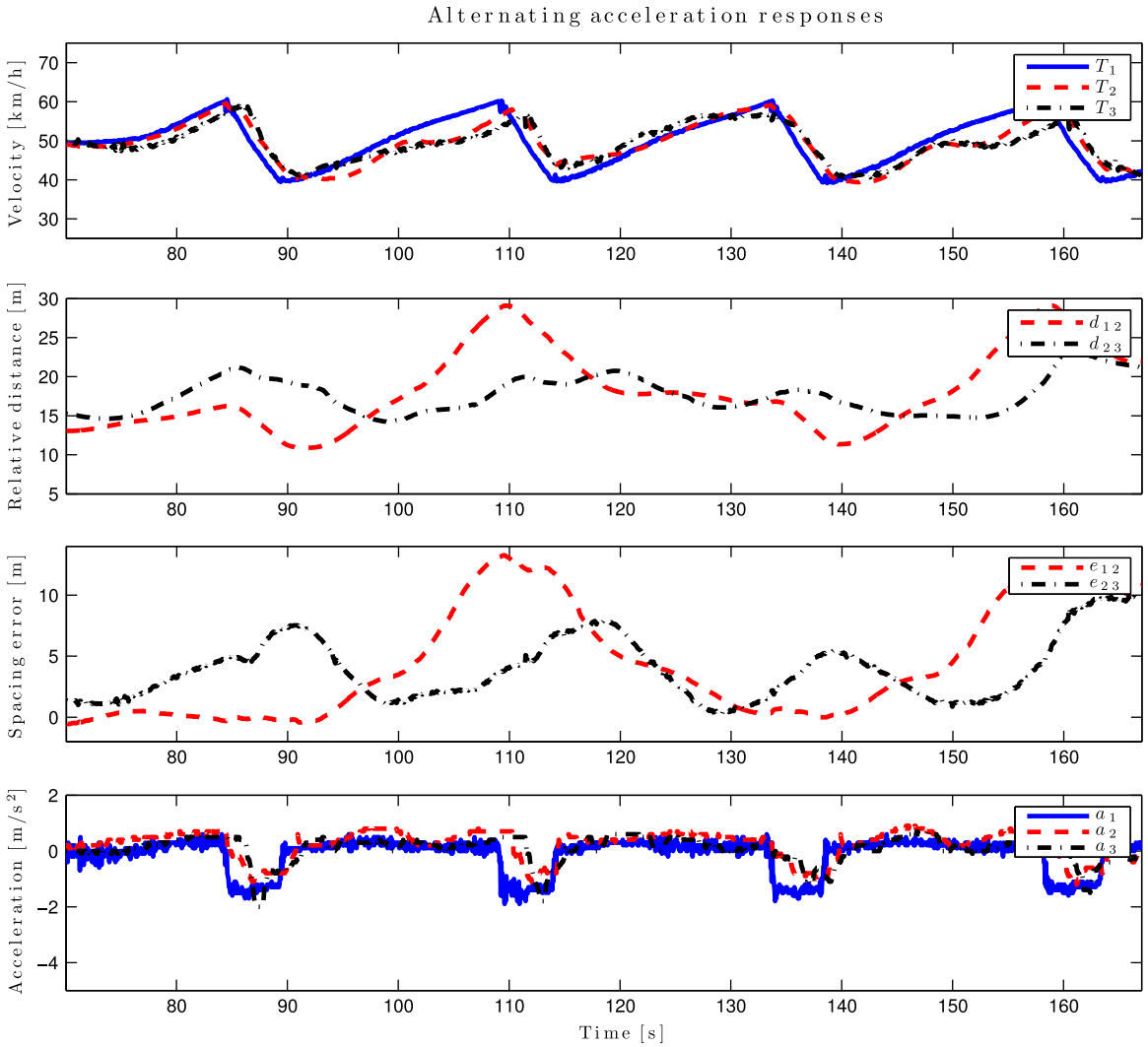

Fig. 11. Experiment results to evaluate the controller performance when the lead vehicle varies its velocity. The solid (blue) lines are the trajectories for the lead vehicle, the (red) dashed lines are the trajectories for the vehicle in the middle, and the (black) dashed-dotted lines are the trajectories for the last vehicle in the platoon. (For interpretation of the references to color in this figure caption, the reader is referred to the web version of this paper.)

errors are attenuated along the chain and they are bounded. The velocity trajectories in the top plot show that there are no over- or under undershoots in velocity. Furthermore, the acceleration trajectories shown in the bottom plot reveal that a slightly harder braking is required for the third vehicle compared to the second vehicle, which is caused by maintaining a more accurate time headway.

7. Conclusions

HDV platooning can be conducted with standardized sensors and control units that are already present on commercial HDVs today. The component that needs to be added is a wireless sensor unit, such that a wider range of information can be shared between the vehicles with low latency. By studying a three-HDV platoon in this paper, we hope to have captured most of the dynamical behavior that occurs in a longer platoon consisting of a lead vehicle, follower vehicles, and a tail-end vehicle. A qualitative study has been presented between a simulation model and real life behavior of an HDV platoon. Even though the results differ to some extent, the simulation model mimics most of the dynamics that are observed in practice. It has been shown, both numerically and through experiments, that the proposed decentralized high-level controller attenuates the disturbances produced by the lead vehicle and operates safely. The smallest deviation from the reference for inter-vehicle spacing was observed to be -1.9 m during a harsh braking. Hence, it can be inferred that the vehicles could have operated at shorter time headways to achieve further air drag reduction, i.e., fuel efficiency, without compromising safety. The controller performs well even though the vehicles operate to some extent outside the equilibrium points. However, there are still nonlinearities present in the system that causes unwanted behavior. In contrast to passenger vehicles, a gear change produced in an HDV has a significant impact on the velocity. We presented a simple model for the EMS and engine dynamics, which worked sufficiently well in most of the studied cases. However, there can still arise cases in the nonlinear engine dynamics that can cause unwanted response delays. These situations do not cause an issue with respect to safety, but degrade the tracking performance and control input energy.

To handle the effects of the observed issues caused by the nonlinearities in engine dynamics, the intention of a necessary gear change could be broadcasted such that the rest of the platooning vehicles will be able to make better informed decisions concerning to change gear simultaneously or to deter the action. Thus, a high-level control law for the gear management system might be necessary to improve the control performance. Furthermore, a more sophisticated

engine model might possibly be required to capture the behavior that affects the tracking performance in a platoon. However, a solution might be to transmit not only the actual velocity of the vehicles in the platoon over the communication network, but also their reference velocity to the EMS. Thereby, each vehicle would be able to determine when the control action to the engine is resumed and increase the turbo pressure to minimize the response delay. Furthermore, a varying steep road grade has a significant effect on the vehicle dynamics, which is not captured in the control design. It will most likely impact the performance. Investigating the mentioned possibilities and the controller performance over a varying road grade requires further experiments and is hence left as future work.

Acknowledgments

This work is partially supported by Scania CV AB, the Swedish Center for Strategic Vehicle Research and Innovation (FFI) and the Swedish Research Council. The authors would also like to extend their gratitude to the senior engineers Henrik Pettersson, Jan Dellrud, Samuel Wickström and Magnus Adolfson, at Scania CV AB, for assisting with the experimental results provided in this paper.

References

Adolfson, M. (January 2014). Cooperative dynamic formation of platoons for safe and energy-optimized goods transportation. In *93rd annual meeting of the transportation research board*, Washington, DC, USA (Oral presentation).

Alam, A. (2011). *Fuel-efficient distributed control for heavy duty vehicle platooning* (Licentiate thesis). Stockholm, Sweden: Royal Institute of Technology.

Alam, A. (2014). *Fuel-efficient heavy-duty vehicle platooning* (Ph.D. thesis). Royal Institute of Technology (KTH).

Alam, A., Gattami, A., & Johansson, K. H. (September 2010). An experimental study on the fuel reduction potential of heavy duty vehicle platooning. In *13th international IEEE conference on intelligent transportation systems*, Madeira, Portugal.

Alam, A., Gattami, A., & Johansson, K. H. (December 2011). Suboptimal decentralized controller design for chain structures: Applications to vehicle formations. In *50th IEEE conference on decision and control and European control conference*, Orlando, FL, USA.

Alam, A., Gattami, A., Johansson, K. H., & Tomlin, C. J. (2014). Guaranteeing safety for heavy duty vehicle platooning: *Safe set computations and experimental evaluations*. *Control Engineering Practice*, *24*(March), 33–41.

Alam, A., Mårtensson, J., & Johansson, K. H. (October 2013). Look-ahead cruise control for heavy duty vehicle platooning. In *16th international IEEE conference on intelligent transportation systems* (pp. 928–935), Hague, The Netherlands.

Åström, K. J. (1970). *Introduction to stochastic control theory*. New York, London: Academic Press.

Åström, K. J., & Hägglund, T. (2006). *Advanced PID control*. New York: ISA—Instrumentation, Systems, and Automation Society. ISBN: 1-55617-942-1.

Barooah, P., Mehta, P. G., & Hespanha, J. P. (2009). Mistuning-based control design to improve closed-loop stability margin of vehicular platoons. *IEEE Transactions on Automatic Control*, *54*(September (9)), 2100–2113.

Bu, F., Tan, H.-S., & Huang, J. (July 2010). Design and field testing of a cooperative adaptive cruise control system. In *American control conference* (pp. 4616–4621) (developed under the California PATH research project).

Chien, C. C., & Ioannou, P. (June 1992). Automatic vehicle-following. In *American control conference* (pp. 1748–1752).

De Schutter, B., Bellemans, T., Logghe, S., Stada, J., De Moor, B., & Immers, B. (1999). Advanced traffic control on highways. *Journal A*, *40*(December (4)), 42–51.

Deutschle, S., Kessler, G. C., Lank, C., Hoffmann, G., Hakenberg, M., & Brummer, M. (April 2010). *Use of electronically linked konvoi truck platoons on motorways*. ATZ autotechnology Edition: 2010-04.

Dunbar, W. B., & Murray, R. M. (2006). Receding horizon control of multi-vehicle formations: *A distributed implementation*. *Automatica*, *42*, 549–558.

European Commission. (2014). *Climate action*. URL: ⟨http://ec.europa.eu/clima/policies/transport/index_en.htm⟩. Accessed February 18, 2014.

Eurostat. (2011). *Energy, transport and environment indicators* (1st ed.). European Union, Luxembourg. ISBN: 978-92-79-21384-7.

Harker, B. J. (September 2001). Promote-chauffeur ii & 5.8 ghz vehicle to vehicle communications system. In *International conference on advanced driver assistance systems* (pp. 81–85) (IEE Conf. Publ. No. 483).

Hedrick, J. K., McMahon, D., Narendran, V., & Swaroop, D. (1991). Longitudinal vehicle controller design for ivhs systems. In *Proceedings of American control conference* (pp. 3107–3112).

Hellström, E. (2010). *Look-ahead control of heavy vehicles* (Ph.D. thesis). Linköping University.

Ioannou, P., & Chien, C. (1993). Autonomous intelligent cruise control. *IEEE Transactions on Vehicular Technology*, *42*(November (4)), 657–672.

Jovanović, M. R., & Bamieh, B. (2004). On the ill-posedness of certain vehicular platoon control problems. In *43rd IEEE Conference on Transportation Research Board annual meeting*. ⟨http://www.trb.org/annualmeeting2014/annualmeeting2014.aspx⟩, Atlantis, Paradise Island, Bahamas.

Kavathekar, P., & Chen, Y. (August 2011). Vehicle platooning: A brief survey and categorization. In *ASME/IEEE international conference on mechatronic and embedded systems and applications, Parts A and B*, Washington, DC, USA.

Kianfar, R., Falcone, P., & Fredriksson, J. (September 2013). A distributed model predictive control (mpc) approach to active steering control of string stable cooperative vehicle platoon. In *7th IFAC symposium on advances in automotive control*, Tokyo, Japan.

Knorn, S., & Middleton, R. H. (July 2013). String stability analysis of a vehicle platoon with communication range 2 using the two-dimensional induced operator norm. In *European control conference* (pp. 3354–3359), Zrich, Switzerland.

Levine, W., & Athans, M. (1966). On the optimal error regulation of a string of moving vehicles. *IEEE Transactions on Automatic Control*, *11*(July (3)), 355–361.

Liang, K., Alam, A., & Gattami, A. (November 2011). The impact of heterogeneity and order in heavy duty vehicle platooning networks. In *3rd IEEE vehicular networking conference*, Amsterdam, Netherlands.

Lidström, K., Sjöberg, K., Holmberg, U., Andersson, J., Bergh, F., Bjäde, M., et al. (2012). A modular CACC system integration and design. *IEEE Transactions on Intelligent Transportation Systems*, *13*(September (3)), 1050–1061.

Mårtensson, J., Alam, A., Behere, S., Khan, M., Kjellberg, J., Liang, K.-Y., et al. (2012). The development of a cooperative heavy-duty vehicle for the GCDC 2011: *Team Scoop*. *IEEE Transactions on Intelligent Transportation Systems*, *13*(September (3)), 1033–1049.

Middleton, R., & Braslavsky, J. (2010). String instability in classes of linear time invariant formation control with limited communication range. *IEEE Transactions on Automatic Control*, *55*(July (7)), 1519–1530.

Milanes, V., Shladover, S., Spring, J., Nowakowski, C., Kawazoe, H., & Nakamura, M. (2014). Cooperative adaptive cruise control in real traffic situations. *IEEE Transactions on Intelligent Transportation Systems*, *15*(February (1)), 296–305.

Naus, G., Vugts, R., Ploeg, J., van de Molengraft, R., & Steinbuch, M. (September 2009). Towards on-the-road implementation of cooperative adaptive cruise control. In *16th world congress on intelligent transport systems and services*, Stockholm, Sweden.

Omae, M., Fukuda, R., Ogitsu, T., & Chiang, W. -P. (September 2013). Spacing control of cooperative adaptive cruise control for heavy-duty vehicles. In *7th IFAC symposium on advances in automotive control*, Tokyo, Japan.

Peppard, L. (1974). String stability of relative-motion pid vehicle control systems. *IEEE Transactions on Automatic Control*, *19*(October (5)), 579–581.

Rajamani, R., Tan, H.-S., Law, B. K., & Zhang, W.-B. (2000). Demonstration of integrated longitudinal and lateral control for the operation of automated vehicles in platoons. *IEEE Transactions on Control Systems Technology*, *8*(July (4)), 695–708.

Rajamani, R., & Zhu, C. (1999). Semi-autonomous adaptive cruise control systems. In *Proceedings of the American control conference* (Vol. 2, pp. 1491–1495), San Diego, CA, USA.

Robinson, T., Chan, E., & Coelingh, E. (October 2010). Operating platoons on public motorways: An introduction to the sartre platooning programme. In *17th world congress on intelligent transport systems*, Busan, Korea.

Rödönyi, G., Gáspár, P., & Bokor, J. (June 2013). Unfalsified uncertainty modeling for computing tight bounds on peak spacing errors in vehicle platoons. In *American control conference* (pp. 3057–3062), Washington, DC, USA.

Sahlholm, P., & Johansson, K. H. (2010). Road grade estimation for look-ahead vehicle control using multiple measurement runs. *Control Engineering Practice*, *18*(11), 1328–1341.

Seiler, P., Pant, A., & Hedrick, J. K. (2004). Disturbance propagation in vehicle strings. *IEEE Transactions on Automatic Control*, *49*(October (10)), 1835–1842.

Shaout, A., & Jarrah, M. A. (1997). Cruise control technology review. *Computers & Electrical Engineering*, *23*(July (4)), 259–271.

Sheikholeslam, S., & Desoer, C. A. (1993). Longitudinal control of a platoon of vehicles with no communication of lead vehicle information: a system level study. *IEEE Transactions on Vehicular Technology*, *42*(November (4)).

Swaroop, D. (1994). *String stability of interconnected system: An application to platooning in automated highway systems* (Ph.D. thesis). University of California at Berkeley.

Swaroop, D., & Hedrick, J. K. (1996). String stability of interconnected systems. *IEEE Transactions on Automatic Control*, *41*(March (3)), 349–357.

Swaroop, D., Hedrick, J. K., Chien, C.C., & Ioannou, P. (1994). A comparison of spacing and headway control laws for automatically controlled vehicles. *Vehicle System Dynamics 23* (1).

Tsugawa, S. (September 2013). An overview on an automated truck platoon within the energy its project. In: *7th IFAC symposium on advances in automotive control*, Tokyo, Japan.

Turri, V., Besselink, B., Mårtensson, J., & Johansson, K. H. (December 2014). Look-ahead control for fuel-efficient heavy-duty vehicle platooning. In *53rd IEEE conference on decision and control*, Los Angeles, CA, USA.

van Nunen, E., Kwakkernaat, R., Ploeg, J., & Netten, B. D. (2012). Cooperative competition for future mobility. *IEEE Transactions on Intelligent Transportation Systems*, *13*(September (3)), 1018–1025.

Yanakiev, D., & Kanellakopoulos, I. (2008). Nonlinear spacing policies for automated heavy-duty vehicles. *IEEE Transactions on vehicular technology*, *47*(November (4)).